Establishment and Characterization of an Embryonic Pericyte Cell Line

Huaning Zhao^{1, 2}, Jordan Darden^{2, 3}, John C. Chappell^{1, 2, 3, 4}

¹Center for Heart and Regenerative Medicine, Virginia Tech Carilion Research Institute, Roanoke, VA 24016, USA

²Department of Biomedical Engineering and Mechanics, ³Graduate Program in Translational Biology, Medicine, and Health, Virginia Polytechnic Institute and State University, Blacksburg, VA 24061, USA

⁴Department of Basic Science Education, Virginia Tech Carilion School of Medicine, Roanoke, VA 24016, USA

Running Title: Pericyte Cell Line Validation

*Corresponding Author: John C. Chappell, Ph.D.

Virginia Tech Carilion Research Institute

2 Riverside Circle

Roanoke, Virginia 24016 Phone: 540-526-2219 Fax: 540-982-3373

E-mail: JChappell@vtc.vt.edu

COI Statement: The authors have declared that no conflict of interest exists.

Abbreviations: NG2: Neural Glial Antigen-2. MEF: Mouse Embryonic Fibroblast.

HUVEC: Human Umbilical Vein Endothelial Cell.

Abstract: 215 words

Manuscript (including Fig Legends, Methods and References): 8149 words

Figures: 7

Supplemental Data: 1 Figure, 5 Movies

ABSTRACT

Objective: Pericytes are specialized perivascular cells embedded within the basement membrane. These cells envelope the abluminal surface of endothelial cells and promote microvessel homeostasis. Recent discoveries of unique pericyte functions, particularly in neural tissues, underscore the need for overcoming existing challenges in establishing a functionally validated pericyte cell line. Here, we present methodologies for addressing these challenges as well as an embryonic pericyte cell line for use with *in vitro* and *ex vivo* experimental models.

Methods: We isolated an enriched population of Neural Glial Antigen-2 (NG2):DsRed+ pericytes from embryonic day 12.5 (E12.5) mice. This pericyte cell line was compared to mouse embryonic fibroblasts (MEFs) with respect to gene expression, cell morphology and migration, and engagement with endothelial cells during junction stabilization and angiogenesis.

Results: NG2+ pericytes displayed gene expression patterns, cell morphology, and 2D migration behaviors distinct from MEFs. In three different vessel formation models, pericytes from this line migrated to and incorporated into developing vessels. When co-cultured with human umbilical vein endothelial cells (HUVECs), these pericytes stimulated more robust VE-Cadherin junctions between HUVECs as compared to MEFs, as well as contributed to HUVEC organization into primitive vascular structures. Conclusions: Our data support use of this pericyte cell line in a broad range of models to further understand pericyte functionality during normal and pathological conditions.

Keywords: pericytes, endothelial cells, mouse embryonic fibroblasts, vascular morphogenesis

INTRODUCTION

Pericytes were first described in the 1870s by Eberth and Rouget as cells morphologically distinct from vascular smooth muscle cells yet occupying the perivascular space adjacent to microvessels. The advent of electron microscopy allowed further characterization of these cells as being embedded within the basement membrane along endothelial cells of the microvasculature [50]. Subsequent studies have since identified a wide range of functions for these cells. It has been well established that pericytes are critical for stabilizing newly formed blood vessels, promoting their maturation while maintaining vessel integrity and barrier function [3,27]. Pericytes also contribute to the extracellular matrix (ECM) and basement membrane composition [2,45]. Pericyte contractility [15,17] and potential modulation of capillary blood flow has also been described [20,42], though the exact nature of their involvement in blood flow regulation remains an open question [23,24]. Additionally, pericytes have been implicated in tissue regeneration through differentiation into a broad range of distinct cell types [13,55]. These established and emerging pericyte functions have generated significant interest in further understanding their roles in blood vessel development, vascular homeostasis, and in various disease conditions.

Pericyte loss or dysfunction contributes to the onset and progression of numerous pathologies. For instance, diabetic retinopathy involves extensive damage of the retina microvasculature including pericyte "dropout", which contributes to vascular instability and unchecked proliferative growth of new vessels [1]. Intraventricular hemorrhage, or

"brain bleeds", in prematurely born infants also arises in part from the inadequate investment of pericytes into the fragile and still-developing vasculature within the neonatal brain [9,62]. Alzheimer's disease and amyotrophic lateral sclerosis (ALS) are also associated with defective pericyte function and coverage [29], as the loss of vascular barrier function contributes to the onset of neuronal dysfunction and neuro-degeneration. Pericytes have been implicated in the pathogenesis of lung and kidney fibrosis [4,32,46], as well as in limiting blood flow restoration following stroke or spinal cord injury [18,20,31]. Tumor vessel dysmorphogenesis also arises in part from the lack of adequate pericyte coverage and investment, which likely contributes to the metastatic potential of a particular tumor type [6,36,63]. Given the involvement of pericytes in such a wide range of clinical pathologies, development of new models and tools to study this cell type during normal and disease conditions is critical.

The experimental approaches for investigating pericyte behavior and function are still being developed and refined, especially relative to the methods used to study their endothelial counterparts. A recent scientific statement from the American Heart Association indicated that major challenges in interpreting observations from *in vitro* angiogenesis assays stem from the lack of pericyte inclusion and the large variability in pericyte sources [49]. This variability is due in part to pericytes often being classified as "mural cells" alongside vascular smooth muscle cells and fibroblasts. Because these cells share some overlapping characteristics and perhaps lineages [25,57], it is critical to continue developing criteria to distinguish these distinct cell populations. For instance, He et al. recently identified enriched expression of vitronectin (*vtn*) and

interferon-induced transmembrane protein 1 (*ifitm1*) as potential pericyte biomarkers [21] in addition to more established, though not exclusive, markers such as neural-glial antigen 2 (NG2, gene: cspg4, chondroitin sulfate proteoglycan-4) and platelet-derived growth factor receptor- β (PDGFR β) [3]. While gene expression profiling represents one modality for refining the selection criteria for a pericyte cell line, additional methods will need to be developed to further validate pericyte cell lines as representative models of their behavior and activity.

In the current study, we combined gene transcription analysis with functional assays to validate a pericyte cell line for use with *in vitro* and *ex vivo* experimental platforms. Specifically, we isolated an enriched population of pericytes from mice at embryonic day 12.5 (E12.5). Pericytes expressed the DsRed fluorescent protein under the ng2 (cspg4) promoter (i.e. NG2:DsRed) [65]. The E12.5 time-point was chosen because neural oligodendrocyte progenitor cells (OPCs), a cell type that also eventually expresses NG2, are not NG2+ until after E13.5 [56]. Pericyte gene expression, cell morphology, and 2D migration dynamics differed significantly from that of E14-15 mouse embryonic fibroblasts (MEFs). In addition, pericytes from this cell line migrated towards angiogenic vessels and incorporated into nascent vascular structures in three different models of blood vessel development. Vascular Endothelial (VE)-Cadherin junctions between endothelial cells were more prominent when co-cultured with pericytes as compared to MEFs. Pericytes also appeared to contribute to endothelial cell organization into primitive vascular structures. Taken together, our data suggest that, in addition to a distinct gene expression profile, this pericyte cell line exhibited functional characteristics

consistent with their expected roles of participating in, and perhaps shaping, blood vessel formation and enhancing endothelial cell junctions.

MATERIALS AND METHODS

Embryo Collection and Pericyte Primary Cell Line Isolation

All animal experiments were conducted with review and approval from the Virginia Tech Institutional Animal Care and Use Committee (IACUC). All protocols are reviewed and approved by the IACUC Board and Virginia Tech Veterinary Staff. The Virginia Tech NIH/PHS Animal Welfare Assurance Number is A-32081-01 (Expires: 7/31/2021). Mice expressing the DsRed fluorescent protein under control of the Ng2 promoter (i.e. Ng2-DsRed mice) [Tg(Cspg4-DsRed.T1)1Akik/J, JAX # 008241, The Jackson Laboratory, Bar Harbor, ME] were set up in timed matings with C57BL/6 females. On embryonic day 12.5 (E12.5), embryos were collected and placed in dissection media at 4°C, and Ng2-DsRed+ embryos were visually identified. Embryonic tissues were enzymatically dissociated in Type I collagenase (2 mg/ml, Fisher) in phosphate buffer saline (PBS) with Ca²⁺ and Mg²⁺ at 37°C for 1 hour. Following centrifugation (3 mins at 1200 rpm), supernatant was removed, and cells were re-suspended in 0.25% Trypsin-EDTA (Life Technologies, Carlsbad, CA) for 10 mins at 37°C. Newborn calf serum was added to neutralize the Trypsin reaction. Following passage through a 70-micron pore filter and centrifugation (5 mins at 1200 rpm), cells were re-suspended in pericyte media (see Supporting Information) and plated for culture and expansion. Confluent cells were washed twice in PBS and exposed to Trypsin-EDTA for 5 mins at 37°C, which was subsequently neutralized with serum. After centrifugation (3 mins, 2000 rpm), dissociated cells were filtered, re-suspended in a buffer suitable for Fluorescence-Activated Cell Sorting (FACS, Sony SH800, San Jose, CA), and placed on ice. FACS gates were set to (i) remove doublets, (ii) exclude Ng2-DsRed negative cells (based on

control cell auto-fluorescence), and (iii) collect cells with the highest DsRed fluorescence intensity. Cells were imaged before and after FACS, and these images were quantified for the level of NG2+ cell enrichment (n=6 randomly chosen fields of view for each group). Collected cells were then cultured in a specific pericyte media, which was designed to promote the survival of pericytes and enrich their numbers at the expense of any other cell types that could have been present. Enriched pericytes were utilized for subsequent experiments between passages 3-6 (p3-6). Cells were maintained under sterile conditions at all times where possible, and were not tested for the presence of mycoplasma.

Comparative Gene Expression, Cell Morphology, and Migration Behavior Gene Expression

Mouse embryonic fibroblasts (MEFs) (Lonza, Walkersville, MD) were cultured according to manufacturer instructions. For comparative gene expression analysis, pericytes and MEFs were digested in lysis buffer (Zymo Research, Irvine, CA) at the same passage number. Messenger RNA was extracted and purified using Quick-RNA MiniPrep kit (Zymo) following manufacturer recommendations. Reverse transcription of RNA to cDNA was achieved using High Capacity cDNA Reverse Transcription Kit (Applied Biosystems, Foster City, CA) reagents and following manufacturer recommendations for PCR. Quantitative PCR was performed in triplicate (n=4 biological replicates) utilizing Taqman® Gene Expression Master Mix (Applied Biosystems) and Taqman® probes for Gene Expression including primers for TATA binding protein (tbp) for normalization, as well as Notch3 (notch3), interferon-induced transmembrane protein

1 (*ifitm1*), vitronectin (*vtn*), fibroblast specific protein-1 (*s100A4*), and fibroblast activation protein (*fap*). Samples were analyzed using standard 96 well plates on a QuantStudio 6 Flex (Applied Biosystems) with QuantStudio $^{\text{TM}}$ Real-Time PCR Software using comparative $\Delta\Delta$ T method to determine expression changes.

Cell Morphology

Morphological differences between pericytes and MEFs were evaluated by culturing each cell type individually on custom-made 6-well glass-bottom plates and by subsequently fixing with 4% paraformaldehyde (PFA) (Electron Microscopy Sciences, Hatfield, PA). Following three PBS rinses, blocking solution [3% bovine serum albumin (BSA) in PBS] was applied for 1 hour. Fixed cells were labeled for fluorescent confocal microscopy through incubation with CytoPainter Phalloidin-iFluor 488 Reagent (Abcam, Cambridge, MA). Primary antibodies against mouse NG2 (rabbit anti-mouse NG2, EMD Millipore, Billerica, MA) were applied, followed by secondary labeling with donkey anti-rabbit AlexaFluor 568 (Invitrogen, Carlsbad, CA). Cell nuclei were labeled with 4′,6-Diamidino-2-phenylindole dihydrochloride (DAPI). Immunostained cells were imaged on a Zeiss LSM 880 confocal microscope (Zeiss, Thornwood, NY) with 2-4 images acquired through the sample thickness, and these z-stack images were compressed into a single image using ImageJ/Fiji [43,47,48] or Zen software (Zeiss).

Migration Behavior

Comparison of pericyte and MEF migration dynamics was conducted by culturing each cell type individually on custom-made 6-well glass-bottom plates. Time-lapse imaging of cell migration was conducted on a Zeiss LSM 880 (Zeiss) mounted with an environmental chamber (regulated CO₂, humidity, and 37°C temperature). Bright-field,

differential interference contrast (DIC), and fluorescent (561 excitation) images were acquired every 10 mins for 24 hours. Cell migration speed was calculated by using ImageJ to measure the displacement of the cell nucleus/centroid at each time step, and these distances were divided by the time interval (n=30 cells for each cell type).

Pericyte-Endothelial Cell Co-culture Dynamics

Human umbilical vein endothelial cells (HUVECs, Lonza, Walkersville, MD) were cultured according to manufacturer instructions in Endothelial Cell Growth Media-2 (EGM2, Lonza, Walkersville, MD). Pericytes or MEFs were added to confluent HUVECs on glass-bottom plates (referred to hereafter as co-cultures) at a ratio of 1:6 (1 pericyte/MEF for every 6 HUVECs) and maintained in EGM-2 exchanged every other day. Brightfield and DIC images of co-cultures were acquired every day, and at days 0, 3, and 6 after co-culture initiation, the apparent surface area of HUVEC regions was measured and averaged for both co-culture groups (i.e. MEF:HUVEC and pericyte:HUVEC, with n=5 randomly chosen fields of view per time point). Approximately 48 hours after adding the second cell type, live imaging of co-cultures was conducted as described above for pericyte/MEF monocultures (i.e. environmental chamber on confocal microscope, 10 min acquisition intervals for 24 hours). Cocultures not used for live imaging experiments were fixed with 4% PFA, washed in PBS (x3), incubated in blocking solution, and labeled as described above (i.e. Phalloidin for actin cytoskeleton, anti-NG2 antibody, and DAPI). In addition, endothelial cell junctions were labeled with a primary antibody against mouse VE-Cadherin (goat anti-mouse VE-Cadherin, Santa Cruz Biotechnology, Dallas, TX), followed by secondary antibody

labeling donkey anti-goat Alexa Fluor 647 (Jackson ImmunoResearch, West Grove, PA). Compressed z-stack images were acquired for each co-culture configuration as described above.

Pericyte Recruitment and Investment in Vessel Formation Assays

Tube Formation in 3D Collagen Matrix

Passage 4-6 HUVECs were cultured alone, with pericytes, or with MEFs (ratio 6:1, that is 6 HUVECs for every 1 pericyte or MEF) in 1x10⁶ cells per ml in Type I collagen (2 mg/mL, Advanced BioMatrix, Carlsbad, CA) in glass-bottom plates. Cells were cultured in EGM2 media with the addition of murine Vascular Endothelial Growth Factor- A (VEGF-A, 30 ng/mL, Peprotech, Rocky Hill, NJ). After 4-6 days, collagen-embedded cells were fixed, stained for VE-Cadherin, NG2, and DAPI, and imaged by confocal microscopy as described above.

Embryonic Stem Cell-Derived Blood Vessels

Wild-type embryonic stem cells (ESCs) [a kind gift from G.H. Fong (University of Connecticut Health Center) and V.L. Bautch (University of North Carolina at Chapel Hill)] were maintained and differentiated into primitive vascular structures as previously described [10,26,40]. "Hanging drops" of ESCs were created to initiate differentiation of embryoid body spheroids. Pericytes were added 7 days following the start of differentiation (i.e. removal from leukemia inhibitory factor, LIF). Day 10 cultures were fixed with 4% PFA and labeled for NG2 and DAPI. In addition, platelet-endothelial cell adhesion molecule-1 (PECAM-1/CD31) was detected with primary antibody labeling against mouse PECAM-1 (rat anti-PECAM-1/CD31, BD Pharmingen/BD Biosciences,

San Diego, CA) and secondary antibody labeling with donkey anti-rat Alexa Fluor 488 (Jackson ImmunoResearch). Compressed z-stack images of primitive vessels with endogenous and exogenous pericytes were acquired as described above.

Embryonic Tissue Culture Assay

Culture of the remodeling vasculature within embryonic back skin was conducted as previously described [10]. Briefly, mice expressing enhanced GFP (eGFP) under control of the *Flk-1* (VEGF Receptor-2) promoter (i.e. *Flk-1-eGFP* mice) [*Kdr*^{tm2.1}*Jrt*/J, JAX #017006, The Jackson Laboratory] were set up in timed matings with C57BL/6 females.

Embryonic back skin was collected from E13.5 *Flk-1-eGFP*+ mice and embedded in fibrin within a single well of a custom-made, glass-bottom 6-well plate [38]. Pericytes (p4-6) were enzymatically dissociated into single cells and re-suspended in basic culture media: Dulbecco's Modified Eagle Medium-High Glucose (DMEM-H, Gibco/Thermo Fisher Scientific, Rockford, IL), 10% Fetal Bovine Serum (FBS, Gibco), and 1% Antibiotic-Antimycotic (Gibco). Following complete polymerization of the fibrin matrix, these cells and media were added on top of the embryonic skin cultures. After 1 hour, remodeling dermal blood vessels and exogenous pericytes were dynamically imaged by confocal microscopy (10× or 20× air objectives) at 20-25 min intervals for 18-24 hours with a Zeiss LSM 880 microscope with full incubation chamber. Z-stacks of 10-14 images were taken for each scan at 4-6 micron intervals, and compressed into a single image at each time point.

Statistics

Statistical analysis was conducted using GraphPad Prism 6 (La Jolla, CA). Where appropriate, statistics were conducted using two-way ANOVA and student t-tests. Relative quantification of qRT-PCR was analyzed by paired two-tailed t-test. P-values less than or equal to 0.05 were considered significant.

RESULTS

Embryonic Tissues Provide a Source for an Enriched Mouse Pericyte Cell Line.

Recent methodological advances have begun to address the wide-range of challenges associated with establishing vascular pericyte cell lines [19,39]. Here, we sought to build upon these approaches by incorporating a pericyte reporter, specifically DsRed expression (i.e. red fluorescence) driven by the promoter of an accepted vascular pericyte marker, NG2 [3,21,65]. Oligodendrocyte progenitor cells (OPCs) in the brain also express Ng2/Cspg4, but no earlier than embryonic day 13.5 (E13.5) [56]; therefore, we collected and dissociated Ng2-DsRed+ embryonic tissues at E12.5 and cultured these cells in pericyte-specific media (Figure 1A). Supplemental Figure 1 of tissue from an E14.5 Flk-1-eGFP; Ng2-DsRed+ littermate demonstrates the abundance and localization of Ng2-DsRed+ cells in embryonic tissues at a comparable time-point. Specific media conditions have been previously shown to effectively select for distinct cell types including pericytes [39], but we sought to accelerate this process by using FACS to isolate and enrich for Ng2-DsRed+ vascular pericytes. Confocal images of sorted cells demonstrated a significant 4-fold enrichment in Ng2-DsRed+ pericytes (Figure 1B-C), such that nearly 70% or greater of the isolated cells were DsRed+, a yield comparable to that achieved with similar approaches for vascular cell isolation [30]. Thus, by combining pericyte-specific media with a genetic reporter and FACS, we were able to utilize mouse embryonic tissues as a viable source for deriving a vascular pericyte cell line for further validation.

Vascular Pericytes and Fibroblasts Exhibit Distinct *In Vitro* Cell Morphologies, Migration Dynamics, and Gene Expression Patterns.

Fibroblasts and pericytes both arise from mesenchymal origins, and although some overlap exists in their morphological features and biomarker expression, these cells perform very distinct functions in their respective tissue compartments. Fibroblasts reside in tissue/organ interstitial space and contribute to connective tissue formation. These cells rarely come in direct contact with the abluminal wall of blood vessels, nor do they become embedded within the vascular basement membrane [44]. Thus, fibroblasts served as a related but distinct cell type for evaluating characteristics of vascular pericytes. We began this comparative analysis by labeling and imaging the actin cytoskeleton (fluorescently-tagged phalloidin) in our pericyte cell line and in commercially available mouse embryonic fibroblasts (MEFs) harvested at a similar point in development, E14-15 (Figure 2A-H). Pericyte cell area appeared larger as compared to MEFs, while the signal from actin stress fiber labeling was weaker and less dense, suggesting fewer and thinner actin filaments (Figure 2A-D). Antibody labeling for NG2 displayed a relatively uniform distribution of the NG2 protein across the plasma membrane. Observations of MEFs revealed cells with stronger and more widespread actin cytoskeleton staining (Figure 2E-H), though some heterogeneity in cell morphology was found, consistent with manufacturer indications of high, though not complete, cell type purity. NG2 antibody labeling was detected primarily around the nucleus in these cells and not extensively along the cell membrane, with some heterogeneity in this distribution pattern.

These distinctions in actin cytoskeleton morphology between the two cell types suggested that the MEFs might be more migratory and thus requiring more robust actin dynamics, while the weaker, sparse actin signal in pericytes suggested a less migratory phenotype [37]. To test this hypothesis, we used live imaging to compare pericyte migration speed relative to that of MEFs. We found that the average pericyte migration speed was significantly lower than MEFs by about 30% (Figure 2I). In addition, approximately 10% of pericytes migrated at or above a speed of 80 microns/hour, while 50% of MEFs migrated at this speed or higher (Figure 2J).

Differences in pericyte and MEF morphology and migration dynamics suggested that these distinct cell types might also exhibit unique transcriptional profiles as well. We explored this idea by applying real-time quantitative reverse transcription PCR (qRT-PCR) to mRNA collected from each cell population. Recent transcriptome profiling studies have identified several novel candidates for exploring pericyte gene expression [21], specifically interferon-induced transmembrane protein 1 (*ifitm1*) and vitronectin (*vtn*) (Figure 2K). We measured expression of these genes as well as more established genes such as Notch3. We also evaluated genes expressed more abundantly in fibroblasts, in particular fibroblast specific protein-1 (*s100A4*), and fibroblast activation protein (*fap*) (Figure 2L). Pericyte expression of *notch3*, *ifitm1*, and *vtn* was significantly higher than MEFs, while the fibroblast-specific gene transcripts were significantly less abundant in the pericytes as compared to the MEFs. These three initial approaches in characterizing this pericyte cell line revealed important morphological and behavioral differences between these cells and fibroblasts, a closely

related but distinct cell type that often confounds identification of pericytes in a range of biological contexts.

Embryonic Pericytes Promote Endothelial Cell Organization into Vessel-like Structures and Enhance VE-Cadherin Junctions.

Pericytes contribute to the blood vessel wall *in vivo* through secretion of extracellular matrix (ECM) components in the basement membrane, as well as by directly engaging the endothelium and promoting junctional stability [58]. As discussed above, fibroblasts do not become embedded in the basement membrane nor do they directly contact endothelial cells under normal physiological conditions. We therefore characterized the unique differences between pericytes and fibroblasts in their interactions with endothelial cells *in vitro* [44]. Culturing our pericyte cell line with human umbilical vein endothelial cells (HUVECs) over several days resulted in the coordination of endothelial cells into more densely populated vessel-like structures (Figure 3A-C). In contrast, HUVECs cultured in the presence of MEFs remained more randomly distributed and spread out, with fibroblasts appearing to extend themselves in between endothelial cells but imparting no apparent organization (Figure 3D-F).

To better understand how pericytes contributed to the observed organization of endothelial cells, we used real-time imaging to visualize dynamic pericyte-endothelial interactions. In tracking pericytes over time, we found that many of these cells appeared to contact multiple endothelial cells along a broad leading edge (black dotted lines in Figure 3G-J, and see Supplemental Movie 1). This edge was maintained by endothelial cell migration and often expanded as time progressed, giving the

appearance of pericytes "pushing" or "shepherding" HUVECs together to establish these denser vessel-like structures. Fibroblasts on the other hand migrated among HUVECs, extending cell processes in between endothelial cells but did not causing HUVECs to aggregate into anything resembling a primitive vascular structure (Figure 3K-N, see Supplemental Movie 2).

We assessed these changes in endothelial cell organization by quantifying the apparent surface area of individual endothelial cells. In doing so, we found that, immediately after adding pericytes to HUVEC cultures, average endothelial cell surface area was larger as compared to the area of endothelial cells cultured with MEFs (Figure 3O). However, after 3 and 6 days in culture with pericytes, HUVECs had significantly smaller individual surface areas as compared to endothelial cells in culture with MEFs. These data were consistent with the time-lapse imaging and longer time-course observations of pericytes inducing endothelial cells to coalesce into primitive vessel-like structures.

In observing endothelial cell aggregation into densely packed, vessel-like structures, we hypothesized that endothelial junctions, specifically those formed by Vascular-Endothelial (VE)-Cadherin, would be more robust in the presence of our pericyte cell line as compared to fibroblasts, perhaps via Neural (N)-Cadherin junction formation between pericytes and endothelial cells [3] or sphingosine-1-phosphate (S1P) signaling [35]. VE-Cadherin junctions between endothelial cells were in fact denser and tightly localized to cell-cell borders in the presence of pericytes, as visualized by confocal microscopy following immunolabeling (Figure 4A-E). Endothelial cells cultured with fibroblasts however had less continuity in their VE-Cadherin junctions, with the

signal being sparser and less associated with cell borders (Figure 4F-J). These observations are well aligned with the known function of pericytes in promoting endothelial cell barrier function.

Isolated Pericytes Engage and Incorporate into Developing Blood Vessels.

Previous studies have shown that mural cell lines can incorporate into the developing vessels in various *in vitro* vasculogenesis and angiogenesis experimental platforms [16,53]. We sought to test the ability of our pericyte cell line to incorporate into blood vessels forming within *in vitro* and *ex vivo* models. We embedded HUVECs in a Type I collagen matrix, and upon VEGF-A stimulation, these endothelial cells formed branched connections, resembling a primitive vascular network (Figure 5A-C). Pericytes added to these 3D cultures behaved similar to the 2D scenario in that individual pericytes engaged numerous endothelial cells along the perimeter of their cell membranes (Figure 5D-F). Fibroblasts cultured with endothelial cells in collagen matrix interacted with HUVECs but rarely contacted several cells along the same edge (Figure 5G-I). In addition, pericytes appeared to be more expansive and have larger projected areas, whereas MEFs were in general thinner and spindly.

Previous observations primarily characterized the differences between the mouse embryonic pericyte cell line and commercially available mouse embryonic fibroblasts. We next utilized a vascular development model in which we could compare the behavior of these isolated and expanded pericytes with that of endogenous pericytes within this vessel formation model. Specifically we released pluripotent mouse embryonic stem cells (ESCs) from an inhibitor of differentiation (i.e. exposure to LIF),

and cultured these cells for 10 days, as described previously [10-12]. During this time, vasculogenic and angiogenic processes give rise to primitive blood vessels including the differentiation, recruitment and investment of vascular pericytes (Figure 6A-D). We took advantage of our pericyte cell line harboring the *Ng2-DsRed* fluorescent reporter, and added these cells to the developing vessels within differentiating ESC cultures. After 3 days, we found that exogenous pericytes had migrated to and begun investing into similar locations as endogenous pericytes, specifically localizing to branch points within the developing vessel-like networks (Figure 6E-H). The functional capacity of these embryonic pericytes was further supported by our observations of their active engagement with the ESC-derived endothelial cells in forming primitive vasculature.

Pericytes are known to migrate alongside endothelial sprouts during angiogenic remodeling [2,60]. We sought to test that functionality of our pericyte cell line by applying them to an *ex vivo* model of blood vessel formation that facilitated real-time imaging of their behaviors. Specifically, we isolated and cultured mouse embryonic skin at E13.5 from mice harboring the *Flk-1-eGFP* reporter gene in vascular endothelial cells [10]. We added *Ng2-DsRed+* pericytes from our cell line to these cultures and observed their migration to and within remodeling vascular networks in real-time (Figure 7A). Exogenous pericytes were able to home to, and initiate contact with, emerging endothelial tip cells (Figure 7B, and see Supplemental Movie 3). In addition, added pericytes tracked along emerging tip cells as they extended from parent vessels and connected to form a new vessel branch (Figure 7C, and see Supplemental Movie 4). The most commonly observed pericyte behavior however was an engagement with the remodeling endothelium (i.e. observable and obvious association) in regions not

necessarily associated with active vessel sprouting (Figure 7D, and see Supplemental Movie 5), suggesting pericyte recruitment might occur via mechanisms in addition to or in conjunction with endothelial tip cell secretion of PDGF-BB [8]. Exogenous pericyte recruitment and migration within vascular networks forming *ex vivo* lends further support for this cell line retaining pericyte functionality during establishment and maintenance as a primary cell line.

DISCUSSION

Vascular pericytes are becoming increasingly implicated in a broad range of physiological and pathological processes, underscoring the need for advancing the tools and models for studying these cells [3,27]. To that end, we isolated a mouse embryonic pericyte cell line and applied a variety of approaches to validate the identity of these cells. Pericyte morphology, migration, and gene expression sharply contrasted with that of mouse embryonic fibroblasts, a cell type of similar mesenchymal lineage but distinct in physiological function and location. Pericyte interactions with endothelial cells were also markedly different from fibroblasts, as pericytes in 2D co-culture promoted formation of vessel-like structures and networks, and in 3D collagen matrices, they maintained contact with multiple endothelial cells simultaneously. When added to vessel formation assays, exogenous pericytes homed to endothelial tip cells as well as branch points within developing networks, and they maintained contact with sprouting endothelial cells as new anastomotic connections formed. These validation steps help address the challenges associated with pericyte source variability [49], which may arise from the current lack of a specific pericyte marker and also from the variety of tissues used for isolating pericytes. These methods may also strengthen interpretations from angiogenesis assays by including a validated pericyte cell line, and at the same time the approaches described herein are yielding new insights into pericyte biology and behaviors, such as pericyte contribution to endothelial cell organization into vessel-like structures.

Pericytes have been described to share a common lineage with a number of cell types including vascular smooth muscle cells and fibroblasts [3,32,33]. While all three

of these cell types have frequently been grouped into the category of "vascular mural cells", each cell type performs very distinct functions in their respective tissue compartments. Validated pericyte cell lines will therefore provide a means to dissect their unique gene expression profiles as well as their individual contributions to vessel structure and homeostasis. Volz et al. recently demonstrated that coronary artery smooth muscle cells arise from pericytes during embryonic development [57]. This study, along with several others, suggests that this overlap in developmental origin may also lead to similar functionality in regulating vessel diameter and tone [20,23], though more work is needed to resolve these potential commonalities across different tissue beds. Regardless of their contractile potential, pericytes, unlike vascular smooth muscle cells, are found deep in the microcirculation, and have been well characterized in promoting vessel barrier function, particularly in the brain [64]. This function contrasts with fibroblasts, which are restricted from residing within the vessel basement membrane [44], and fibroblast-endothelial cell contact has been linked to increased vessel permeability for immune cell extravasation in the lung [59] and increased tissue fibrosis in lung and kidney pathologies [4,32,46,51]. Endothelial cells co-cultured with our pericyte cell line had enhanced VE-Cadherin junctions, while co-culture with fibroblasts led to disrupted endothelial cell junctions. Live imaging of these two coculture scenarios was inline with these endothelial cell junction observations, as pericytes appeared to promote endothelial cell organization and association. In contrast, fibroblasts frequently inserted cellular extensions in between neighboring endothelial cells, consistent with the idea that fibroblasts support endothelial cells, and overall vascular network formation, in a paracrine manner [38,41,61] and less so through direct

contact with the endothelium. Thus, an important criterion for evaluating pericyte cell lines will likely be their function in enhancing endothelial cell junctions and promoting endothelial cell aggregation, which are likely distinct functions relative to other "vascular mural cells".

The de novo formation of primitive vascular networks during vasculogenesis involves endothelial cell differentiation and aggregation, and ultimately organization into basic vessel structures [14]. Pericyte involvement in this process has previously been assumed to be minimal aside from early stabilization of nascent blood vessels [5,34,52]. Our observations of pericyte-endothelial cell co-cultures suggest that pericytes may be participating in rudimentary organization of endothelial cells. Additionally, live imaging of these interactions revealed pericytes maintaining contact with multiple endothelial cells over time and seeming to "push" them together. We have recently observed a similar phenomenon in real-time imaging of an embryonic stem cell (ESC) model in which fluorescently labeled pericytes migrate towards and initiate contact with eGFP+ endothelial cells as they begin organizing into primitive vessel-like structures (L.B. Payne, unpublished observations). Taken together, these data support the idea that pericytes, or perhaps their precursors, may play a more active role in the earliest stages of blood vessel formation, in addition to their roles in vessel stabilization and maturation at later stages.

Recent observations from our lab and others suggest that vascular pericytes are present at the leading edge of a sprouting vascular front, such as in the mouse postnatal retina, and likely engage tip cells as they emerge from existing vessels [28,60]. Sprouting endothelial tip cells are enriched for the expression of PDGF-BB [22], which is

a critical recruitment factor for attracting pericytes to the developing vasculature [53]. By adding exogenous pericytes to the remodeling vessels *ex vivo*, we were able to observe the earliest events in pericyte-endothelial cell interactions as the two cell types initiate contact and begin migrating in a coordinated fashion. This coordinated migration was also observed in pericytes that tracked closely behind endothelial tip cells as they sprouted outward from existing vessels, and even as they form new anastomotic connections. Observing pericytes maintaining such close proximity to sprouting tip cells is therefore consistent with a primary function of pericytes in regulating the stability of nascent vessel branches. Incorporating this validated pericyte cell line into angiogenesis assays will facilitate identification of the mechanisms underlying this coordinated migration of sprouting endothelial cells and tip cell-associated pericytes.

Pericytes have been implicated in the onset and progression of several vascularrelated diseases [7,20,64], with diabetic retinopathy being one of the clearest examples
of pericyte contribution to clinical pathogenesis [1]. In diabetic retinopathy, the vascular
basement membrane thickens [54] (likely in part from pericyte contribution to ECM
deposition [45]), and pericytes are lost via vessel detachment and/or cell death.
Interestingly, we found that exogenous pericytes within the intact vessel networks of
explanted embryonic skin were often limited in their direct engagement with the
endothelium (Figure 7D), except for the tip cell interactions discussed above or at
locations where the basement membrane was likely disrupted. These results, coupled
with observations from the diabetic retina [54] as well as from our own experiments (H.
Zhao, unpublished observations), suggest that the basement membrane, and its ECM
composition in particular, limits the ability of pericytes to attach to endothelial cells. If

the vascular basement membrane does indeed function as a potential "barrier" between the vessel wall and interstitial cells, this may represent an important therapeutic target for clinical strategies aimed at promoting vessel stability and maturation by restoring sufficient pericyte coverage.

While the cell line and validation approaches described in the current study address several of the existing challenges in establishing a functionally validated pericyte cell line, important limitations must also be considered. For instance, to minimize the complexity in presenting multiple cell line comparisons, we did not include commercially available pericytes in our analysis, though future studies will do so. These commercial cell lines are largely from adult specimen and from a variety of tissue types and organs [49], which would likely introduce numerous confounding factors that would require additional analysis beyond the scope of the current study. In addition, we did not exhaustively exclude the possibility that our cell line might represent, or contain small sub-populations of, other cell types including mesenchymal stem cells [13,55]. While our approaches demonstrated that the embryonic pericyte cell line exhibited behaviors consistent with a vascular pericyte identity, we cannot rule out the potential heterogeneity in cell identity within these NG2+ cells. Future work will be needed to determine if such heterogeneity in cell type exists within our cell line and, if so, the relative contributions of each subpopulation.

New roles and functions for vascular pericytes are continuing to emerge, and these cells are becoming increasingly appreciated for their importance in the onset and progression of a wide range of pathological conditions including diabetic retinopathy, Alzheimer's disease, tumor formation and metastasis, among many others. It is

therefore imperative that we develop new tools and models to better understand the basic biology of these cells as well as to elucidate how they might be therapeutically targeted during disease.

PERSPECTIVES

Vascular pericytes are an essential cell type for stabilizing growing vascular networks and maintaining blood vessel health. New tools and methodologies to investigate pericyte biology, such as the ones presented here, are therefore critical for advancing our understanding of pericyte-endothelial cell interactions during normal and pathological conditions. In addition to migration along angiogenic vessels and enhancing endothelial cell junctions, we observed unique contributions of embryonic pericytes to endothelial cell organization into primitive vascular structures, highlighting the need for further studies into the various roles that pericytes play in blood vessel formation and homeostasis.

Acknowledgements

We thank the Chappell Lab for critical and extensive discussions of the primary data.

Sources of Funding.

This work was supported by NIH grants R00HL105779 and R56HL133826 (to JCC).

Disclosures.

None

FIGURE LEGENDS

Figure 1. Embryo-derived *Ng2:DsRed+* cell populations before and after enrichment by FACS. Brightfield (left) and fluorescence (right) images of cells acquired immediately following embryo dissociation (**A**) and after enrichment by FACS (**B**). Scale bars, 100 μm. Average percentages of *Ng2:DsRed*-positive cells per total cell number. n=6 randomly chosen fields of view for each group. Values are averages + Standard Error of the Mean (SEM) (**C**).

Figure 2. Mouse embryonic pericytes exhibit unique cell morphologies, migration dynamics, and gene expression compared to fibroblasts. Representative images of pericytes (A-D) and fibroblasts (E-H) labeled for actin cytoskeleton (A & E, Phalloidin-AlexaFluor488, green in D & H), NG2 expression (B & F, DsRed Reporter or NG2 Ab, red in D & H), and cell nuclei (C & G, DAPI, blue in D & H). Scale bars, 50 μm.

Asterisks mark pericytes in A-D, while asterisks in E-H mark the predominant MEF population and arrowheads label a subtype of MEFs present in these cultures. (I)

Average cell migration speeds (μm/hr) for pericytes (red bars) and MEFs (blue bars).

Values are averages + SEM, n=30 cells. *P<0.05. (J) Distribution of pericyte and MEF migration speeds (μm/hr) across the indicated ranges. (K-L) Fold changes in gene expression between pericytes and MEFs. Values are averages + SEM, n=4 biological replicates. *P<0.05.

Figure 3. Pericytes influence endothelial cell organization during long- and shortterm co-culture, in contrast with MEFs, which allow greater endothelial cell

spreading. Representative phase contrast images of HUVECs in co-culture with pericytes (A-C) and MEFs (D-F) at day 0 (A & D), 3 (B & E), and 6 (C & F). White dashed lines in B and C denote regions where pericytes have excluded HUVECs. Scale bars, 100 μm. Representative frames from short-term live imaging of HUVECs co-cultured with pericytes (G-J) and MEFs (K-N). Black dashed lines in G-J denote the broad leading edge of a pericyte (marked by an asterisk) contacting multiple endothelial cells, while the fibroblast marked by an asterisk in K-N inserts between endothelial cells. Scale bars, 100 μm in G-J, and 50 μm in K-N. Time in upper right corner, hours:minutes (hh:mm). See Supplemental Movies 1 & 2 for full time-course sequences. Average surface area of HUVEC regions at day 0, 3, and 6 of co-culture with pericytes (red bars) and MEFs (blue bars). Values are averages + SEM, n=5 randomly chosen fields of view per time point, *P<0.05.

Figure 4. HUVEC junctions are more robust during co-culture with pericytes as compared to MEFs. Representative images of HUVECs co-cultured with MEFs (A-D) and pericytes (E-H). HUVEC cell-cell junctions labeled by antibodies against VE-Cadherin (A & E, yellow in D & H). Pericyte and MEF expression of NG2 detected by antibody staining (B, red in D) or by DsRed expression (F, red in H), respectively. Cell nuclei labeled by DAPI (C & G, blue in D & H). Scale bars, 50 μm.

Figure 5. Pericytes engage endothelial cells forming primitive vascular structures within a type I collagen matrix *in vitro*. Representative images of HUVECs cultured in a type I collagen matrix alone (**A-D**), with pericytes (**E-H**), or with MEFs (**I-L**). VE-

Cadherin junctions between HUVECs labeled by antibodies (**A**, **E**, **& I**, green in **D**, **H**, **& L**). Pericyte and MEF expression of NG2 detected by antibody staining (**B**, **F**, **& J**, red in **D**, **H**, **& L**). Cell nuclei labeled by DAPI (**C**, **G**, **& K**, blue in **D**, **H**, **& L**). Scale bars, 50 µm.

Figure 6. Exogenous pericytes interact with embryonic stem cell-derived vessels similar to endogenous pericytes. Representative images of mouse embryonic stem cell-derived vessels after 10 days of differentiation, and in association with endogenous pericytes (A-D) or exogenous pericytes added during vessel formation (E-H). Endothelial cells antibody labeled for PECAM-1 (A & E, green in D & H). Pericyte expression of NG2 detected by antibody staining (B, red in D) or by DsRed expression (F, red in H), respectively. Cell nuclei labeled by DAPI (C & G, blue in D & H). Scale bars, 25 μm in A-D, and 50 μm in E-H.

Figure 7. Exogenous pericytes associate with distinct regions of developing blood vessels forming *ex vivo* in explanted embryonic skin. Schematic of experimental design in which live imaging captured *Ng2-DsRed+* pericyte interactions with remodeling vessels within explanted skin of embryonic day 13.5 (E13.5) *Flk-1-eGFP+* mice (**A**). Representative sequential images from movies of exogenous pericytes (*Ng2-DsRed+*) engaging with embryonic skin vessels (*Flk-1-eGFP+*): (i) as a tip cell sprouted from a parent vessel (**B**, arrowheads indicate pericyte extensions; see associated Supplemental Movie 3.), (ii) during endothelial sprout extension and connection (arrows) (**C**, arrowheads indicate pericyte extensions; see associated

Supplemental Movie 4), and (iii) as vessels remodeled without overt sprouting ($\bf D$, arrowheads indicate migrating pericytes; see associated Supplemental Movie 5). Scale bars, 25 μ m in $\bf B$, 100 μ m in $\bf C$, and 50 μ m in $\bf D$. Time in upper right corner, hours:minutes (hh:mm).

REFERENCES

- 1. Antonetti DA, Klein R, Gardner TW. Diabetic retinopathy. *N Engl J Med* **366**: 1227-1239, 2012.
- 2. Armulik A, Abramsson A, Betsholtz C. Endothelial/pericyte interactions. *Circ Res* **97**: 512-523, 2005.
- 3. Armulik A, Genove G, Betsholtz C. Pericytes: developmental, physiological, and pathological perspectives, problems, and promises. *Dev Cell* **21**: 193-215, 2011.
- 4. Barron L, Gharib SA, Duffield JS. Lung Pericytes and Resident Fibroblasts: Busy Multitaskers. *Am J Pathol* **186**: 2519-2531, 2016.
- 5. Bergers G, Song S. The role of pericytes in blood-vessel formation and maintenance. *Neuro-oncology* **7**: 452-464, 2005.
- 6. Bergers G, Song S, Meyer-Morse N, Bergsland E, Hanahan D. Benefits of targeting both pericytes and endothelial cells in the tumor vasculature with kinase inhibitors. *J Clin Invest* **111**: 1287-1295, 2003.
- 7. Birbrair A, Zhang T, Wang ZM, Messi ML, Mintz A, Delbono O. Pericytes at the intersection between tissue regeneration and pathology. *Clin Sci (Lond)* **128**: 81-93, 2015.
- 8. Bjarnegard M, Enge M, Norlin J, Gustafsdottir S, Fredriksson S, Abramsson A, Takemoto M, Gustafsson E, Fassler R, Betsholtz C. Endothelium-specific ablation of PDGFB leads to pericyte loss and glomerular, cardiac and placental abnormalities. *Development* **131**: 1847-1857, 2004.
- 9. Braun A, Xu H, Hu F, Kocherlakota P, Siegel D, Chander P, Ungvari Z, Csiszar A, Nedergaard M, Ballabh P. Paucity of pericytes in germinal matrix vasculature of premature infants. *J Neurosci* **27**: 12012-12024, 2007.
- 10. Chappell JC, Cluceru JG, Nesmith JE, Mouillesseaux KP, Bradley V, Hartland C, Hashambhoy-Ramsay YL, Walpole J, Peirce SM, Gabhann FM, Bautch VL. Flt-1 (VEGFR-1) Coordinates Discrete Stages of Blood Vessel Formation. *Cardiovasc Res* **111**: 84-93, 2016.
- 11. Chappell JC, Mouillesseaux KP, Bautch VL. Flt-1 (Vascular Endothelial Growth Factor Receptor-1) Is Essential for the Vascular Endothelial Growth Factor-Notch

Feedback Loop During Angiogenesis. *Arterioscler Thromb Vasc Biol* **33**: 1952-1959, 2013.

- 12. Chappell JC, Taylor SM, Ferrara N, Bautch VL. Local guidance of emerging vessel sprouts requires soluble Flt-1. *Dev Cell* **17**: 377-386, 2009.
- 13. Diaz-Flores L, Gutierrez R, Madrid JF, Varela H, Valladares F, Acosta E, Martin-Vasallo P, Diaz-Flores L, Jr. Pericytes. Morphofunction, interactions and pathology in a quiescent and activated mesenchymal cell niche. *Histol Histopathol* **24**: 909-969, 2009.
- 14. Drake CJ, Fleming PA. Vasculogenesis in the day 6.5 to 9.5 mouse embryo. *Blood* **95**: 1671-1679, 2000.
- 15. Durham JT, Dulmovits BM, Cronk SM, Sheets AR, Herman IM. Pericyte chemomechanics and the angiogenic switch: insights into the pathogenesis of proliferative diabetic retinopathy? *Invest Ophthalmol Vis Sci* **56**: 3441-3459, 2015.
- 16. Eglinger J, Karsjens H, Lammert E. Quantitative assessment of angiogenesis and pericyte coverage in human cell-derived vascular sprouts. *Inflammation and Regeneration* **37**: 2, 2017.
- 17. Fernandez-Klett F, Offenhauser N, Dirnagl U, Priller J, Lindauer U. Pericytes in capillaries are contractile in vivo, but arterioles mediate functional hyperemia in the mouse brain. *Proc Natl Acad Sci U S A* **107**: 22290-22295, 2010.
- 18. Fernandez-Klett F, Potas JR, Hilpert D, Blazej K, Radke J, Huck J, Engel O, Stenzel W, Genove G, Priller J. Early loss of pericytes and perivascular stromal cell-induced scar formation after stroke. *J Cereb Blood Flow Metab* **33**: 428-439, 2013.
- 19. Greenwood-Goodwin M, Yang J, Hassanipour M, Larocca D. A novel lineage restricted, pericyte-like cell line isolated from human embryonic stem cells. *Sci Rep* **6**: 24403, 2016.
- 20. Hall CN, Reynell C, Gesslein B, Hamilton NB, Mishra A, Sutherland BA, O'Farrell FM, Buchan AM, Lauritzen M, Attwell D. Capillary pericytes regulate cerebral blood flow in health and disease. *Nature* **508**: 55-60, 2014.
- 21. He L, Vanlandewijck M, Raschperger E, Andaloussi Mae M, Jung B, Lebouvier T, Ando K, Hofmann J, Keller A, Betsholtz C. Analysis of the brain mural cell transcriptome. *Sci Rep* **6**: 35108, 2016.

22. Hellstrom M, Phng LK, Hofmann JJ, Wallgard E, Coultas L, Lindblom P, Alva J, Nilsson AK, Karlsson L, Gaiano N, Yoon K, Rossant J, Iruela-Arispe ML, Kalen M, Gerhardt H, Betsholtz C. Dll4 signalling through Notch1 regulates formation of tip cells during angiogenesis. *Nature* **445**: 776-780, 2007.

- 23. Hill RA, Tong L, Yuan P, Murikinati S, Gupta S, Grutzendler J. Regional Blood Flow in the Normal and Ischemic Brain Is Controlled by Arteriolar Smooth Muscle Cell Contractility and Not by Capillary Pericytes. *Neuron* 87: 95-110, 2015.
- 24. Hillman EM. Coupling mechanism and significance of the BOLD signal: a status report. *Annu Rev Neurosci* **37**: 161-181, 2014.
- 25. Hosaka K, Yang Y, Seki T, Fischer C, Dubey O, Fredlund E, Hartman J, Religa P, Morikawa H, Ishii Y, Sasahara M, Larsson O, Cossu G, Cao R, Lim S, Cao Y. Pericyte-fibroblast transition promotes tumor growth and metastasis. *Proc Natl Acad Sci U S A* **113**: E5618-5627, 2016.
- 26. Kearney JB, Bautch VL. In vitro differentiation of mouse ES cells: hematopoietic and vascular development. *Methods Enzymol* **365**: 83-98, 2003.
- 27. Kelly-Goss MR, Sweat RS, Stapor PC, Peirce SM, Murfee WL. Targeting pericytes for angiogenic therapies. *Microcirculation* **21**: 345-357, 2014.
- 28. Kofler NM, Cuervo H, Uh MK, Murtomaki A, Kitajewski J. Combined deficiency of Notch1 and Notch3 causes pericyte dysfunction, models CADASIL, and results in arteriovenous malformations. *Sci Rep* **5**: 16449, 2015.
- 29. Lange S, Trost A, Tempfer H, Bauer HC, Bauer H, Rohde E, Reitsamer HA, Franklin RJ, Aigner L, Rivera FJ. Brain pericyte plasticity as a potential drug target in CNS repair. *Drug Discov Today* **18**: 456-463, 2013.
- 30. Levenberg S, Ferreira LS, Chen-Konak L, Kraehenbuehl TP, Langer R. Isolation, differentiation and characterization of vascular cells derived from human embryonic stem cells. *Nat Protoc* **5**: 1115-1126, 2010.
- 31. Li Y, Lucas-Osma AM, Black S, Bandet MV, Stephens MJ, Vavrek R, Sanelli L, Fenrich KK, Di Narzo AF, Dracheva S, Winship IR, Fouad K, Bennett DJ. Pericytes impair capillary blood flow and motor function after chronic spinal cord injury. *Nat Med* **23**: 733-741, 2017.

32. Lin SL, Kisseleva T, Brenner DA, Duffield JS. Pericytes and perivascular fibroblasts are the primary source of collagen-producing cells in obstructive fibrosis of the kidney. *Am J Pathol* **173**: 1617-1627, 2008.

- 33. Majesky MW, Dong XR, Regan JN, Hoglund VJ. Vascular smooth muscle progenitor cells: building and repairing blood vessels. *Circ Res* **108**: 365-377, 2011.
- 34. Marmé D, Fusenig NE. *Tumor angiogenesis : basic mechanisms and cancer therapy*edn. New York: Springer, 2008.
- 35. McGuire PG, Rangasamy S, Maestas J, Das A. Pericyte-derived sphingosine 1-phosphate induces the expression of adhesion proteins and modulates the retinal endothelial cell barrier. *Arterioscler Thromb Vasc Biol* **31**: e107-115, 2011.
- 36. Morikawa S, Baluk P, Kaidoh T, Haskell A, Jain RK, McDonald DM. Abnormalities in pericytes on blood vessels and endothelial sprouts in tumors. *Am J Pathol* **160**: 985-1000, 2002.
- 37. Murray D, Horgan G, Macmathuna P, Doran P. NET1-mediated RhoA activation facilitates lysophosphatidic acid-induced cell migration and invasion in gastric cancer. *Br J Cancer* **99**: 1322-1329, 2008.
- 38. Nakatsu MN, Hughes CC. An optimized three-dimensional in vitro model for the analysis of angiogenesis. *Methods Enzymol* **443**: 65-82, 2008.
- 39. Neng L, Zhang W, Hassan A, Zemla M, Kachelmeier A, Fridberger A, Auer M, Shi X. Isolation and culture of endothelial cells, pericytes and perivascular resident macrophage-like melanocytes from the young mouse ear. *Nat Protoc* **8**: 709-720, 2013.
- 40. Nesmith JE, Chappell JC, Cluceru JG, Bautch VL. Blood vessel anastomosis is spatially regulated by Flt1 during angiogenesis. *Development* **144**: 889-896, 2017.
- 41. Newman AC, Nakatsu MN, Chou W, Gershon PD, Hughes CC. The requirement for fibroblasts in angiogenesis: fibroblast-derived matrix proteins are essential for endothelial cell lumen formation. *Mol Biol Cell* **22**: 3791-3800, 2011.
- 42. Peppiatt CM, Howarth C, Mobbs P, Attwell D. Bidirectional control of CNS capillary diameter by pericytes. *Nature* **443**: 700-704, 2006.

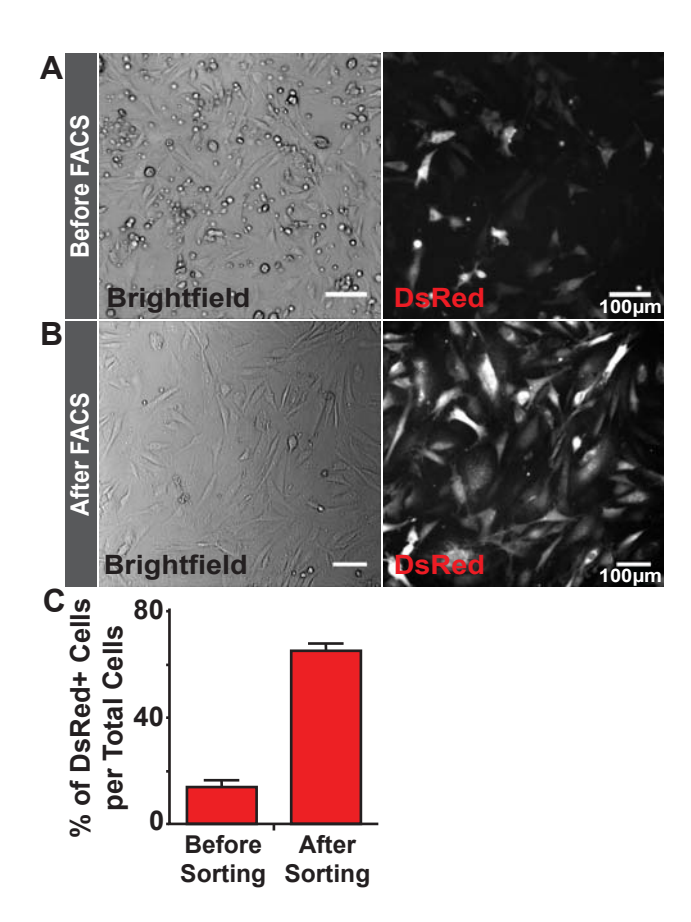
43. Rasband WS. ImageJ, U.S. National Institutes of Health, Bethesda, Maryland, USA. http://rsb.info.nih.gov/ij/, 1997-2012.

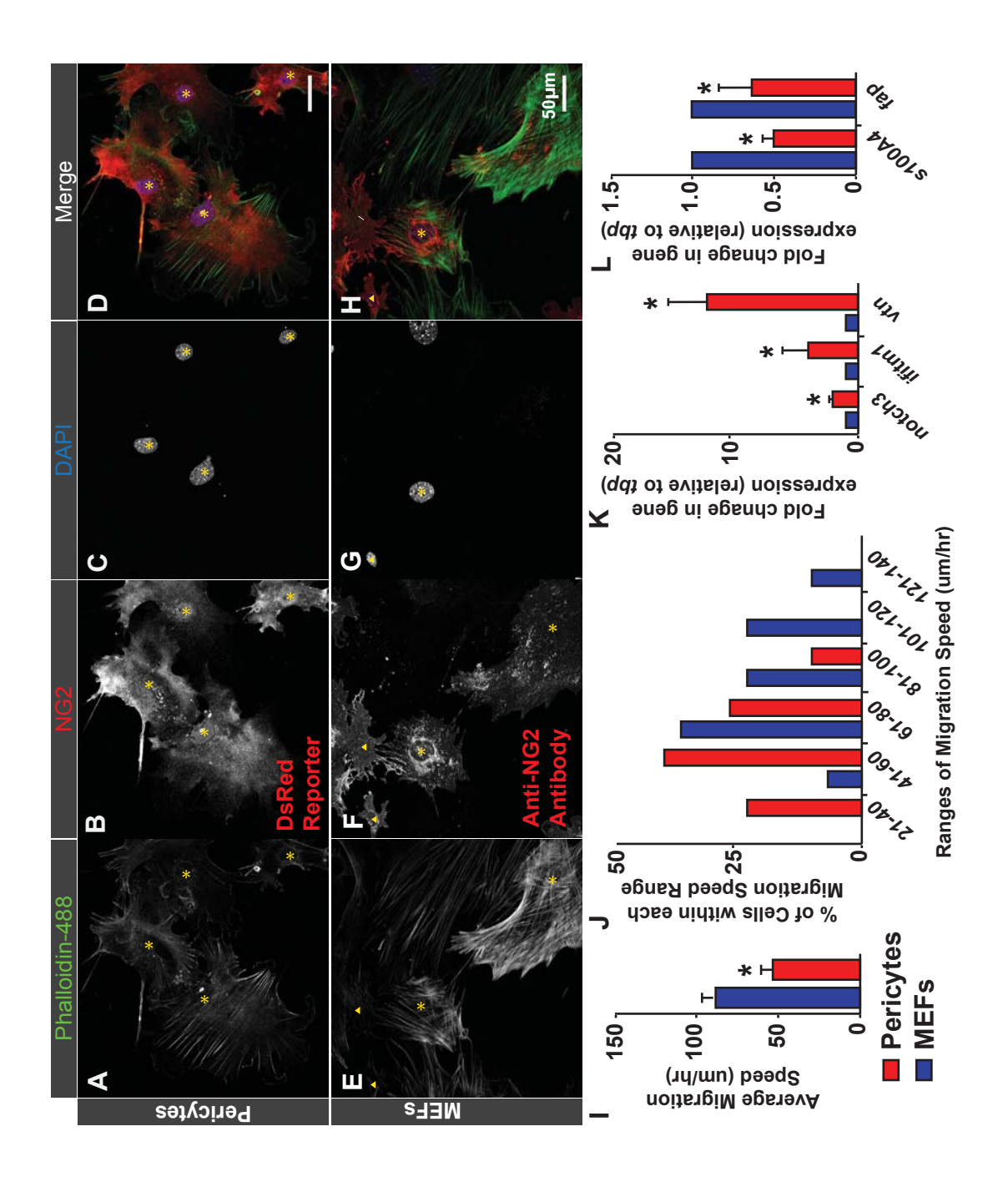
- 44. Rock JR, Barkauskas CE, Cronce MJ, Xue Y, Harris JR, Liang J, Noble PW, Hogan BL. Multiple stromal populations contribute to pulmonary fibrosis without evidence for epithelial to mesenchymal transition. *Proc Natl Acad Sci U S A* **108**: E1475-1483, 2011.
- 45. Sava P, Cook IO, Mahal RS, Gonzalez AL. Human microvascular pericyte basement membrane remodeling regulates neutrophil recruitment. *Microcirculation* **22**: 54-67, 2015.
- 46. Sava P, Ramanathan A, Dobronyi A, Peng X, Sun H, Ledesma-Mendoza A, Herzog EL, Gonzalez AL. Human pericytes adopt myofibroblast properties in the microenvironment of the IPF lung. *JCI Insight* **2**, 2017.
- 47. Schindelin J, Arganda-Carreras I, Frise E, Kaynig V, Longair M, Pietzsch T, Preibisch S, Rueden C, Saalfeld S, Schmid B, Tinevez JY, White DJ, Hartenstein V, Eliceiri K, Tomancak P, Cardona A. Fiji: an open-source platform for biological-image analysis. *Nature methods* **9**: 676-682, 2012.
- 48. Schneider CA, Rasband WS, Eliceiri KW. NIH Image to ImageJ: 25 years of image analysis. *Nature methods* **9**: 671-675, 2012.
- 49. Simons M, Alitalo K, Annex BH, Augustin HG, Beam C, Berk BC, Byzova T, Carmeliet P, Chilian W, Cooke JP, Davis GE, Eichmann A, Iruela-Arispe ML, Keshet E, Sinusas AJ, Ruhrberg C, Woo YJ, Dimmeler S, American Heart Association Council on Basic Cardiovascular S, Council on Cardiovascular S, Anesthesia. State-of-the-Art Methods for Evaluation of Angiogenesis and Tissue Vascularization: A Scientific Statement From the American Heart Association. *Circ Res* **116**: e99-132, 2015.
- 50. Sims DE. The pericyte--a review. *Tissue Cell* **18**: 153-174, 1986.
- 51. Stefanska A, Eng D, Kaverina N, Duffield JS, Pippin JW, Rabinovitch P, Shankland SJ. Interstitial pericytes decrease in aged mouse kidneys. *Aging (Albany NY)* **7**: 370-382, 2015.
- 52. Stratman AN, Malotte KM, Mahan RD, Davis MJ, Davis GE. Pericyte recruitment during vasculogenic tube assembly stimulates endothelial basement membrane matrix formation. *Blood* **114**: 5091-5101, 2009.

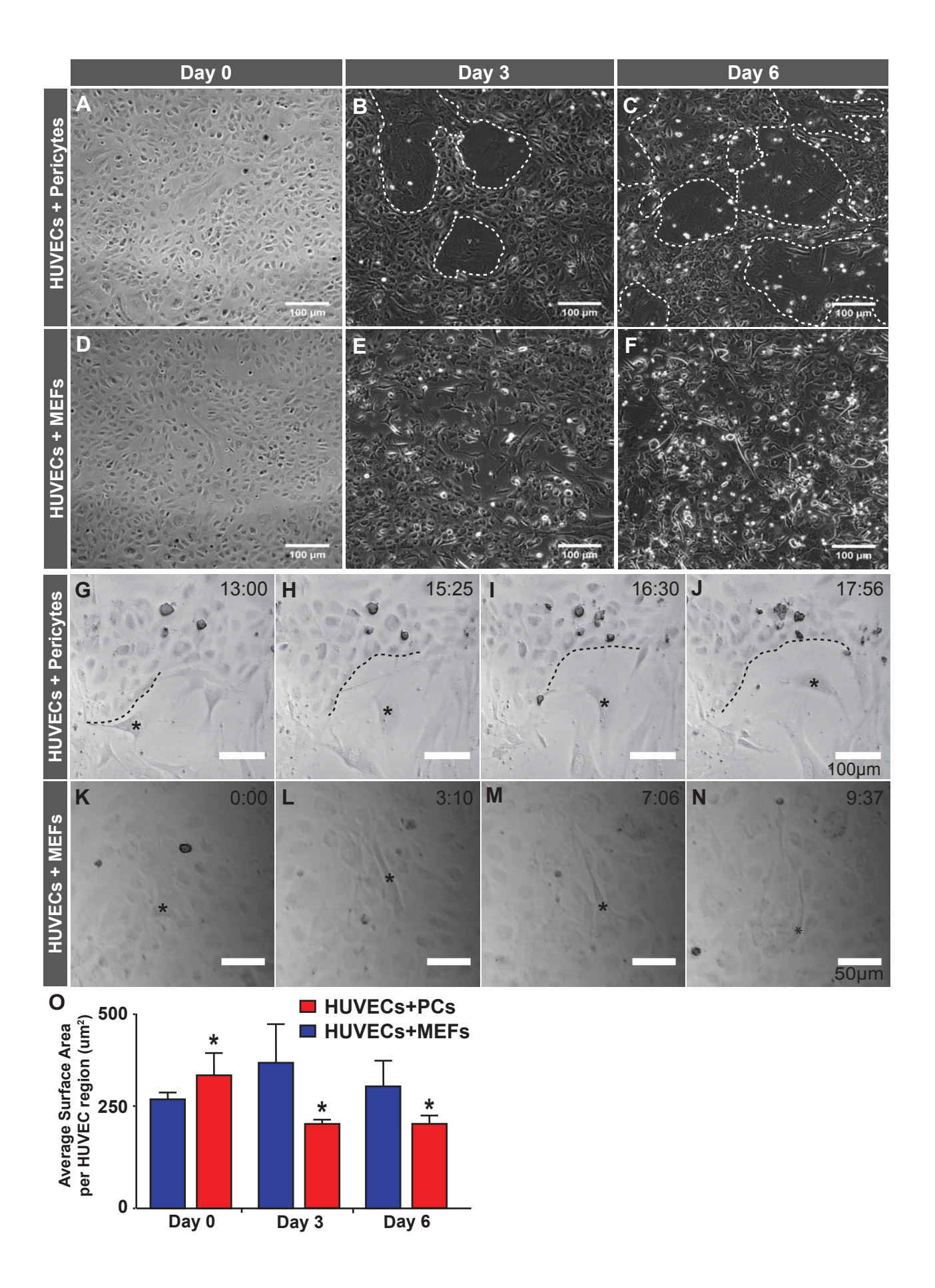
- 53. Stratman AN, Schwindt AE, Malotte KM, Davis GE. Endothelial-derived PDGF-BB and HB-EGF coordinately regulate pericyte recruitment during vasculogenic tube assembly and stabilization. *Blood* **116**: 4720-4730, 2010.
- 54. To M, Goz A, Camenzind L, Oertle P, Candiello J, Sullivan M, Henrich PB, Loparic M, Safi F, Eller A, Halfter W. Diabetes-induced morphological, biomechanical, and compositional changes in ocular basement membranes. *Exp Eye Res* **116**: 298-307, 2013.
- 55. Trost A, Lange S, Schroedl F, Bruckner D, Motloch KA, Bogner B, Kaser-Eichberger A, Strohmaier C, Runge C, Aigner L, Rivera FJ, Reitsamer HA. Brain and Retinal Pericytes: Origin, Function and Role. *Front Cell Neurosci* **10**: 20, 2016.
- 56. Trotter J, Karram K, Nishiyama A. NG2 cells: Properties, progeny and origin. *Brain Res Rev* **63**: 72-82, 2010.
- 57. Volz KS, Jacobs AH, Chen HI, Poduri A, McKay AS, Riordan DP, Kofler N, Kitajewski J, Weissman I, Red-Horse K. Pericytes are progenitors for coronary artery smooth muscle. *Elife* **4**, 2015.
- 58. von Tell D, Armulik A, Betsholtz C. Pericytes and vascular stability. *Exp Cell Res* **312**: 623-629, 2006.
- 59. Walker DC, Behzad AR, Chu F. Neutrophil migration through preexisting holes in the basal laminae of alveolar capillaries and epithelium during streptococcal pneumonia. *Microvasc Res* **50**: 397-416, 1995.
- 60. Walpole J, Gabhann FM, Peirce SM, Chappell JC. Agent-based Computational Model of Retinal Angiogenesis Simulates Microvascular Network Morphology as a Function of Pericyte Coverage. *Microcirculation*, 2017.
- 61. Whisler JA, Chen MB, Kamm RD. Control of perfusable microvascular network morphology using a multiculture microfluidic system. *Tissue Eng Part C Methods* **20**: 543-552, 2014.
- 62. Yang D, Baumann JM, Sun YY, Tang M, Dunn RS, Akeson AL, Kernie SG, Kallapur S, Lindquist DM, Huang EJ, Potter SS, Liang HC, Kuan CY. Overexpression of vascular endothelial growth factor in the germinal matrix induces neurovascular proteases and intraventricular hemorrhage. *Sci Transl Med* **5**: 193ra190, 2013.

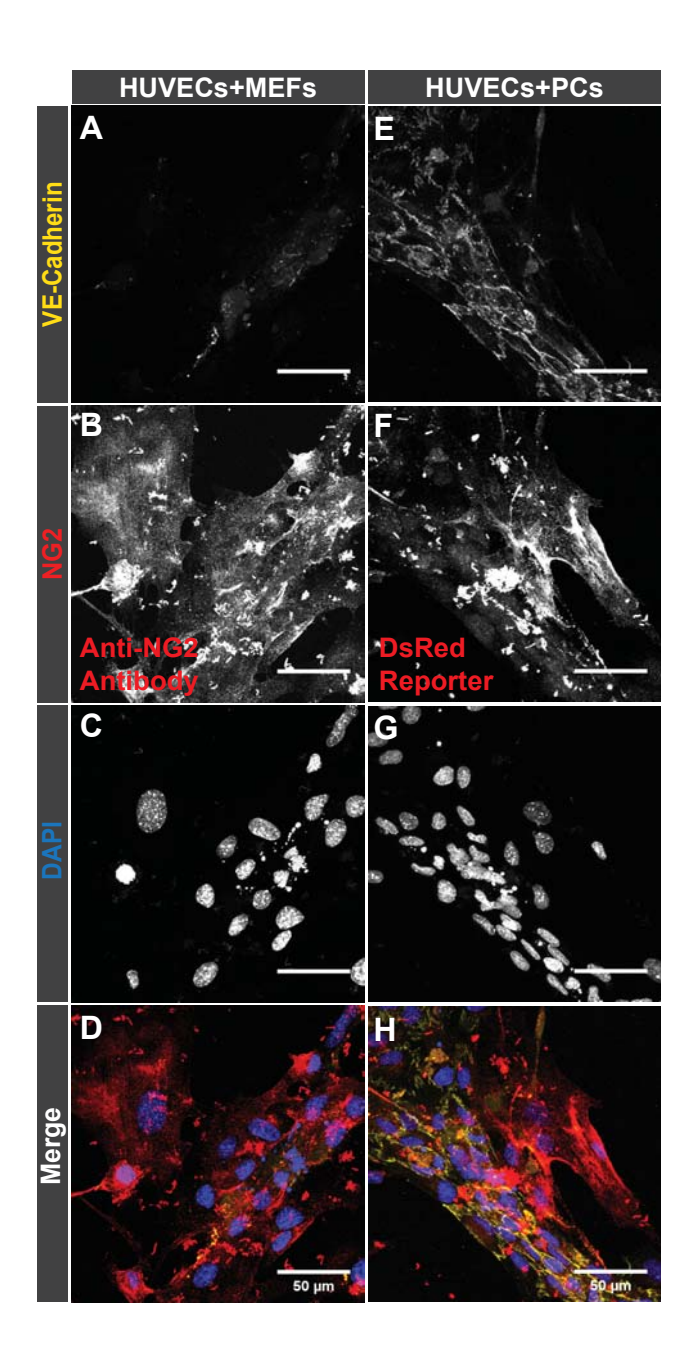
63. Yonenaga Y, Mori A, Onodera H, Yasuda S, Oe H, Fujimoto A, Tachibana T, Imamura M. Absence of smooth muscle actin-positive pericyte coverage of tumor vessels correlates with hematogenous metastasis and prognosis of colorectal cancer patients. *Oncology* **69**: 159-166, 2005.

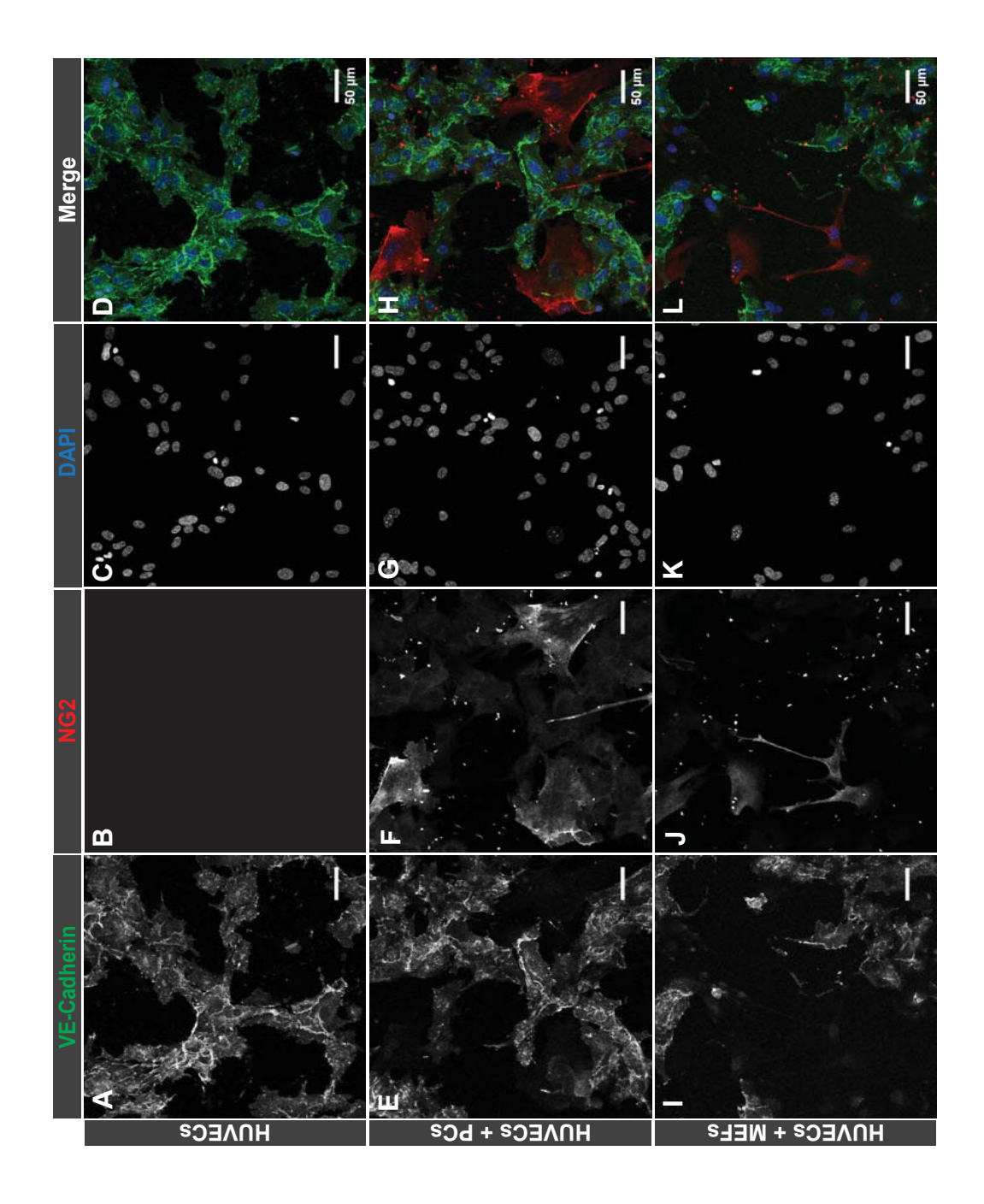
- 64. Zhao Z, Nelson AR, Betsholtz C, Zlokovic BV. Establishment and Dysfunction of the Blood-Brain Barrier. *Cell* **163**: 1064-1078, 2015.
- 65. Zhu X, Bergles DE, Nishiyama A. NG2 cells generate both oligodendrocytes and gray matter astrocytes. *Development* **135**: 145-157, 2008.

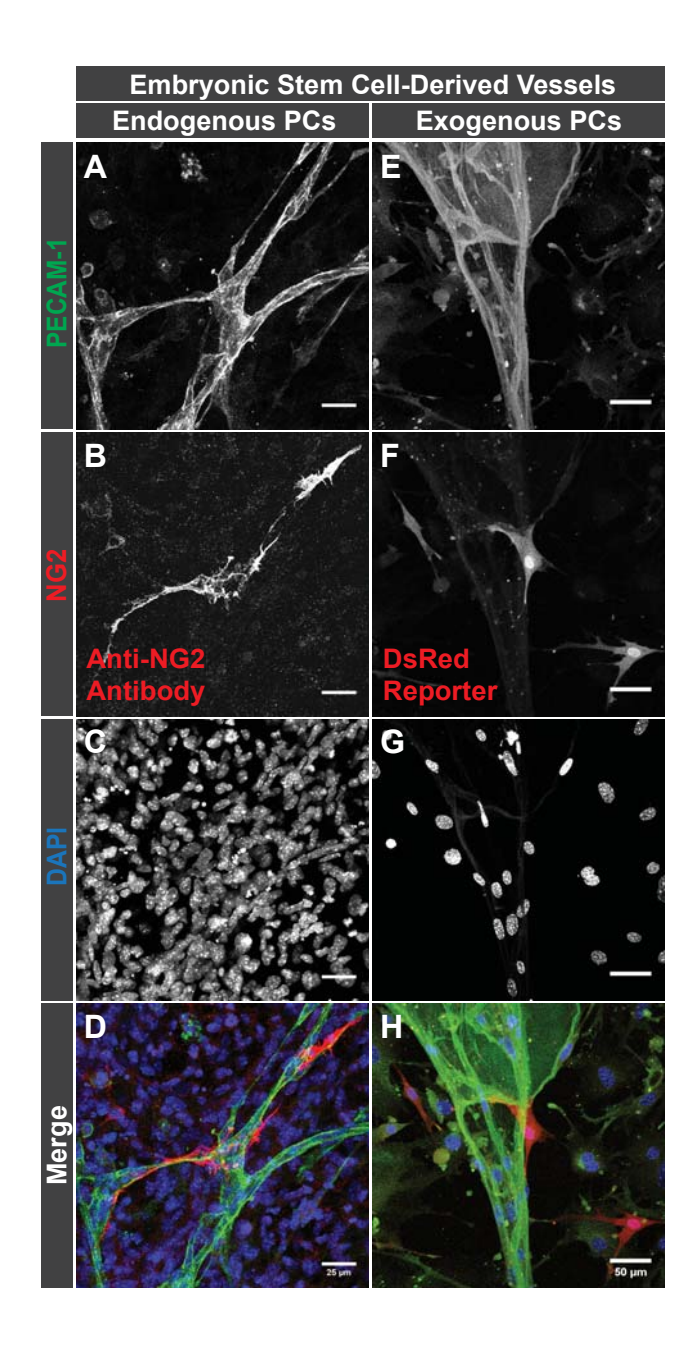


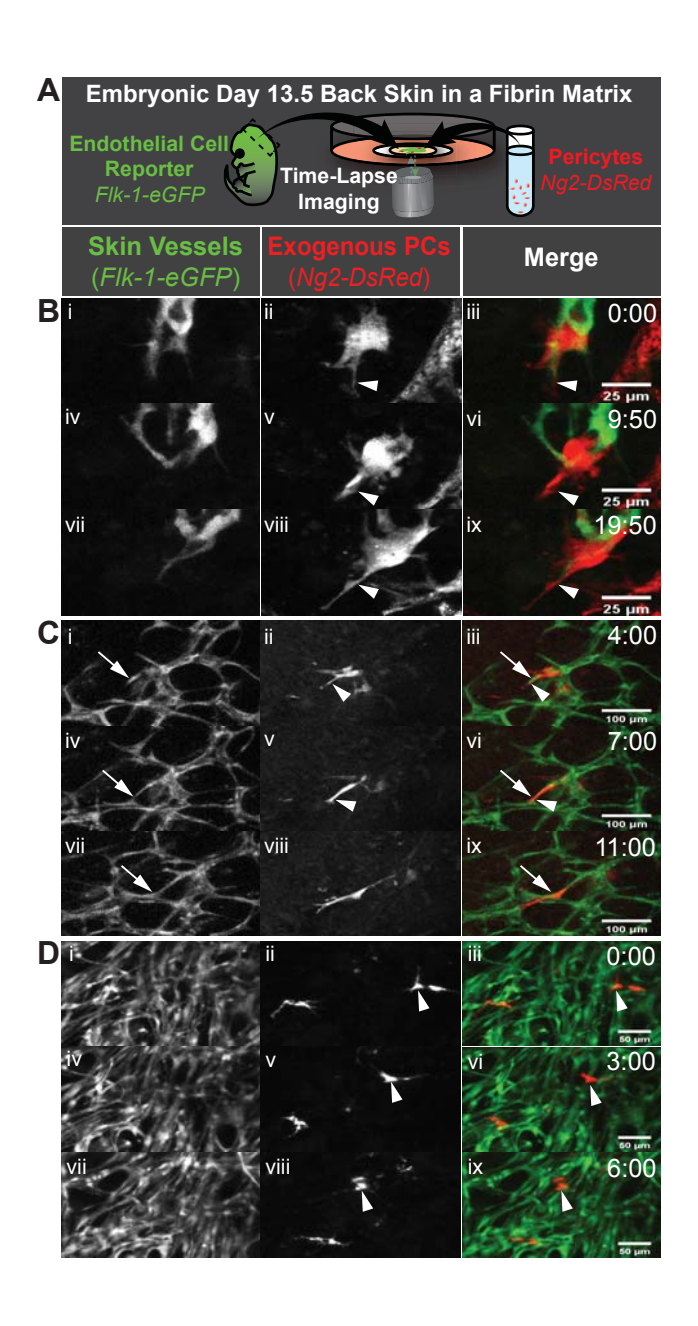












Establishment and Characterization of an Embryonic Pericyte Cell Line SI MATERIALS AND METHODS

Cell Culture and Maintenance

Each cell line was maintained using a distinct media formulation, as detailed below:

- Human umbilical vein endothelial cells (HUVECs) ECM Media (per 500 mL):
 EGM-2 kit components including antibiotics (Lonza) with 450 mL DMEM-L (low
 glucose at 1 g/L, Life Technologies) and 10% fetal bovine serum (FBS) (Life
 Technologies).
- Pericyte (PC) cell line PC media (per 500 mL): 450 mL DMEM-L (Life
 Technologies), 10% FBS (Life Technologies), 1% L-glutamine (Sigma), 1% Antibiotic & Anti-mycotic (Life Technologies), 0.1 ng/mL Sodium Heparin (Sigma), 1
 ng/mL basic Fibroblast Growth Factor (bFGF/FGF-2) (Life Technologies), 1 ng/mL
 Recombinant Murine VEGF165 (Peprotech).
- Mouse Embryonic Fibroblast (MEFs) cell line MEF media (per 500 mL): 450 mL
 DMEM-L (Life Technologies), 10% FBS (Life Technologies), 1% Anti-biotic & Anti-mycotic (Life Technologies).

Endothelial Cell Co-Cultures and Live Imaging

HUVECs were seeded at 2,500 cells/cm² on glass-bottom dishes (gel-coated) and cultured in ECM media for 6-10 days. Pericytes or MEFs were added at the ratio 1:6 (PC or MEF:HUVEC) when HUVECs reached confluence. Co-cultures were dynamically imaged as follows: confocal images (10× or 20× objectives) were acquired at 10-30 min intervals for 16-24 hours on a Zeiss LSM 880 confocal configured for live imaging (environmental chamber maintained humidity, 5% CO₂, and 37°C). Image stacks of 6-8 images were acquired through

the z-axis (thickness) for each scan with 4-6 microns between focal planes. After acquisition, z-stacks were compressed into a single image for each time point. Representative movie sequences shown are from non-consecutive images.

Live Imaging of Pericytes added to ex vivo Embryonic Skin Culture

Animal experiments were conducted with approval from the Virginia Tech Institutional Animal Care and Use Committee (IACUC). All protocols were reviewed and approved by the IACUC Board and Virginia Tech Veterinary Staff. The Virginia Tech NIH/PHS Animal Welfare Assurance Number is A-32081-01 (Expires: 7/31/2021). Culture and dynamic imaging of remodeling vasculature within embryonic back skin was conducted as previously described¹. Briefly, mice with enhanced GFP (eGFP) expression under control of the Flk-1 (VEGF Receptor-2) promoter (i.e. Flk-1-eGFP mice) [Kdr^{tm2.1Jrt}/J, JAX #017006, The Jackson Laboratory] were set up in timed matings with WT females. Back skin was collected from E13.5 Flk-1-eGFP+ mice and embedded in a fibrin gel within one well of a custom-made, glass-bottom 6-well plate². Enzymatically dissociated pericytes (passage 4-6) were resuspended in PC culture media (described above). Fibrin gel was composed of bovine fibringen (2 mg/mL, VWR), 10% Aprotinin from bovine lung (Sigma), and 1% Thrombin from bovine plasma (Sigma). Following complete polymerization of the fibrin matrix, pericytes and media were added on top of the embryonic skin cultures. After 1 hour, remodeling skin blood vessels and exogenous pericytes were dynamically imaged by confocal microscopy (10× or 20× air objectives) at 20-30 min intervals for 18-24 hours with a Zeiss LSM 880 microscope with full incubation chamber. Z-stacks of 10-14 images were taken for each scan at 4-6 micron intervals, and compressed into a single image at each time point.

FIGURE LEGEND

Supplemental Figure 1. Tissue from an E14.5 *Flk-1-eGFP*; *Ng2-DsRed* mouse demonstrates the extent of vessel coverage by *Ng2-DsRed*+ pericytes. Representative images of *Flk-1-eGFP*+ endothelial cells and *NG2-dsRed*+ pericytes from E14.5 embryonic back skin (**A-D**). Scale bars, 200 μm (in **A** and **C**) and 100 μm (in **B** and **D**). *Flk-1-eGFP*+ endothelial cells (image **i** in **A-D**, and green in image **iii** of **A-D**) form extensive networks covered by vascular pericytes (image **ii** in **A-D**, and red in image **iii** of **A-D**).

MOVIE LEGENDS

Supplemental Movie 1. From *Figure 3G-J* of the main paper. Time sequence of HUVECs in co-culture with pericytes. Time in upper right corner, hh:mm (hours:minutes). Scale bar, 100 μm.

Supplemental Movie 2. From *Figure 3K-N* of the main paper. Time sequence of HUVECs in co-culture with MEFs. Time in upper right corner, hh:mm (hours:minutes). Scale bar, 50 μm.

Supplemental Movie 3. From *Figure 7B* of the main paper. Time sequence of exogenous pericytes (red, *Ng2-DsRed+*) engaging with a *Flk-1-eGFP+* endothelial sprout (green) emerging form a parent vessel within cultured E13.5 embryonic skin. Time in upper right corner, hh:mm (hours:minutes). Scale bar, 25 μm.

Supplemental Movie 4. From *Figure 7C* of the main paper. Time sequence of exogenous pericytes (red, *Ng2-DsRed*) tracking along an *Flk-1-eGFP*+ endothelial cell sprout (green) as

it extends from a parent vessel and connects to form a new vessel branch. Time in upper right corner, hh:mm (hours:minutes). Scale bar, 100 μ m.

Supplemental Movie 5. From *Figure 7D* of the main paper. Time sequence of exogenous pericytes (red, Ng2-DsRed+) engaged the remodeling endothelium (green, Flk-1-eGFP+) in regions without appreciable vessel sprouting. Time in upper right corner, hh:mm (hours:minutes). Scale bar, 50 μ m.

REFERENCES

- 1. Chappell JC, Cluceru JG, Nesmith JE, Mouillesseaux KP, Bradley V, Hartland C, Hashambhoy-Ramsay YL, Walpole J, Peirce SM, Gabhann FM, Bautch VL. Flt-1 (VEGFR-1) Coordinates Discrete Stages of Blood Vessel Formation. *Cardiovasc Res* 2016;**111**:84-93.
- 2. Nakatsu MN, Hughes CC. An optimized three-dimensional in vitro model for the analysis of angiogenesis. *Methods Enzymol* 2008;**443**:65-82.

